RESEARCH COMMUNICATION

Repression of the heavy ferritin chain increases the labile iron pool of human K562 cells

Or KAKHLON*†, Yosef GRUENBAUM† and Z. Ioav CABANTCHIK*[1]

*Department of Biological Chemistry, Institute of Life Sciences, Hebrew University, Jerusalem 91904, Israel, and †Department of Genetics, Institute of Life Sciences, Hebrew University, Jerusalem 91904, Israel

The role of ferritin in the modulation of the labile iron pool was examined by repressing the heavy subunit of ferritin in K562 cells transfected with an antisense construct. Repression of the heavy ferritin subunit evoked an increase in the chemical levels and pro-oxidant activity of the labile iron pool and, in turn, caused a reduced expression of transferrin receptors and increased expression of the light ferritin subunit

Key words: antisense, fluorescence detection of metals, transfection.

INTRODUCTION

The expression of ferritin, the major intracellular iron-storage protein, is thought to have two principal regulatory functions, which involve scavenging of intracellular iron and the attenuation of reactive oxygen species (ROS) formation. In the first, synthesis of ferritin subunits is triggered by a rise in the putative cellular labile iron pool (LIP) that is sensed and transduced by iron-responsive proteins (IRPs). In the second, ferritin transcription is modulated in response to factors that either raise or lower cellular growth-dependence on LIP. Thus oncogene suppression of ferritin expression purportedly raises the LIP and supports proliferation [1–6]. On the other hand, cytokines, by promoting ferritin expression and thereby lowering the LIP, confer upon cells protection from invading pathogens and oxidative damage [7–11].

Thus far, experimental support for the alleged role of ferritin in the control of LIP levels has been provided only by studies of heavy ferritin subunit (H-FT) overexpression. In these studies [12,13], expression of the *H-FT* gene mutated in the iron-responsive element enabled the iron-independent translation of H-FT. This strategy led to an increased expression of H-FT which, in turn, reduced the steady-state LIP levels and the ensuing ROS production, and increased resistance to ROS toxicity [13]. Furthermore, stable inducible transfection of HeLa cells with wild-type H-FT cDNA, but not with its ferroxidase mutant, led to a substantial reduction in the LIP [14]. This reduction was associated with up-regulation of IRP activity, transferrin-mediated iron uptake and resistance to ROS toxicity.

In the present study, we analysed the opposite situation, i.e. the functional consequences of H-FT repression in terms of its capacity to increase the LIP. For that purpose, we used transient transfection of cells with an antisense sequence against H-FT as a means to down-modulate expression of H-FT. The choice of antisense was made in order to manipulate ferritin in a specific manner, and independently of the iron status of the cells. The specificity of the antisense H-FT was confirmed by its inability to repress light ferritin subunit (L-FT). We used fluorescence detection of metals as a means to assess LIP [15], and the oxidation of carboxydichlorodihydrofluorescin (carboxy-H_2DCF) as a means to assess exogenously induced ROS production [16]. The levels of cell-surface expression of the transferrin receptor (TfR) served as a tool for confirming the iron-regulation capacity of LIP. Our results provide direct experimental support for the alleged roles of H-FT as a regulator of LIP and as an attenuating factor in the antioxidative cell response.

EXPERIMENTAL

Materials

Calcein, calcein acetomethoxy, 2′-7′-carboxydichlorodihydrofluorescein-diacetate diacetoxymethyl ester (H_2DCFDA-diAM) and fluorescein-β-galactosidase were obtained from Molecular Probes (Eugene, OR, U.S.A.), and Triton X-100 and the DOTAP lipid reagent were from Boehringer Mannheim. The following gifts were received: human H-FT cDNA and rabbit anti-human sera against placental and spleen ferritin from Professor H. Rosen and Professor A. M. Konijn respectively (Hadassah Medical School, Hebrew University), salicylaldehyde hydrazone from Professor Prem Ponka (McGill University, Montreal, Canada), mouse anti-(human H-FT) and anti-(human L-FT) monoclonal antibodies and recombinant human H-FT and L-FT from Dr Paolo Santambroggio (Dipartimento di Ricerca Biologica e Technologica, San Rafaelle Hospital, Milan, Italy), and the pRBG4 vector from Dr Israel Seckler (Faculty of Medicine, Ben Gurion University, Beer Sheva, Israel). Unless specified otherwise, all other chemicals were from Sigma or were of the best available grade.

Cells

Human erythroleukaemia K562 cells were grown as described in [17].

Transient transfection of cells with antisense to ferritin mRNAs

A partial human H-FT cDNA sequence (residues 283–616 in human H-FT mRNA sequence, GenBank® accession number L20941) was PCR-synthesized using the primers 5′-GGAACA-TGCTGAGAAACTG-3′ (forward) and 5′-GGTGTGCTTGT-CAAAG-3′ (reverse). An *Eco*RI recognition sequence, 5′-CCG-

Abbreviations used: H-FT, heavy ferritin subunit; L-FT, light ferritin subunit; LIP, labile iron pool; ROS, reactive oxygen species; TfR, transferrin receptor; IRP, iron-responsive protein; RT, reverse transcriptase; DAPI, 4,6-diamidino-2-phenylindole; carboxy-H_2DCF, carboxydichlorodihydrofluorescin; H_2DCFDA-diAM, 2′-7′-carboxydichlorodihydrofluorescein-diacetate diacetoxymethyl ester.

[1] To whom correspondence should be addressed (e-mail ioav@cc.huji.ac.il).

GAATTCC-3′, was added to the 5′ of each primer and used for ligation in an antisense orientation between the promoter and the polyadenylated sequences of the cytomegalovirus in the pRBG4 vector [18]. The antisense orientation was verified by sequencing the insert and junction sequences. Transfection of pRBG4 with and without the H-FT antisense insert was done by the DOTAP method (Boehringer Mannheim) and assessed 24 h later.

Ferritin quantitation by ELISA

For ferritin determination, samples of approx. 400000 cells were centrifuged, and the pellet was extracted at 4 °C for 15 min with 200 μl of buffer (10 mM Tris/HCl, pH 7.4, 150 mM NaCl, 0.3 % Triton X-100 and 0.25 % NaN_3) containing an antiprotease cocktail (P-8340; Sigma) and 250 μM PMSF. The extract was centrifuged at 8500 ***g*** for 2 min at 4 °C, and the supernatant was analysed for protein content (bicinchoninic acid method; Sigma). Immunoplates (Nunc, Roskilde, Denmark) were coated with mouse anti-(human H-FT) or mouse anti-(human L-FT) monoclonal antibodies (20 μg/ml in carbonate buffer, pH 9.6) and incubated for 1 h at 37 °C. The plates were then blocked with 3 % BSA in PBS for 2 h at room temperature. Subsequently, samples (2 μg of protein) and ferritin standards (0–1 ng of recombinant H-FT or L-FT) were dissolved in 3 % BSA and added to the plates for incubation of 1 h at 37 °C. Incubation (3 h at room temperature) with rabbit antisera against human placental ferritin (approx. 50 % anti-H-FT and 50 % anti-L-FT activity) or against human spleen ferritin (95 % anti-L-FT and 5 % anti-H-FT activity) was used for determination of H-FT and L-FT respectively. Rabbit IgG was detected by incubation with goat anti-rabbit antibodies coupled to β-galactosidase (Amersham International) for 1 h at 37 °C and then 1 h at room temperature. Fluorescence ($\lambda_{excitation}$ 488 nm; $\lambda_{emission}$ 525 nm) of the fluorogenic substrate fluorescein-β-galactosidase was followed with time of incubation in a Fluostar II fluorescence plate reader (BMG LabTechnologies, GmBH, Offenburg, Germany) and quantified with the aid of calibration curves of normal rabbit IgG.

Assessment of RNA levels of H-FT and L7 by reverse transcriptase (RT)-PCR

Total RNA from K562 cells was isolated using Ultraspec RNA isolation reagent (Biotec Laboratories, Houston, TX, U.S.A.). RNA (1 μg) was reverse-transcribed and PCR amplified using the Titan One Step RT-PCR system according to the manufacturer's instructions (Roche Diagnostics, Mannheim, Germany). Total RNA was added to the PCR mix (containing avian myeloblastosis virus RT, *Taq* and *Pwo* DNA polymerases and 40 units/μl RNase inhibitor) together with the following primer pairs. For human H-FT (GenBank® accession number L20941): forward, 5′-GCCAAATACTTTCTTCACC-3′; reverse, 5′-TTCATTATCACTGTCTCCC-3′. These primers spanned a 390 bp sequence between residues 365 and 754. For human L7 (an internal control, GenBank® accession number X57958): forward, 5′-GAAGAGAAGAAGAAGGAGG-3′; reverse, 5′-GGTACATAGAAGTTGCCAG-3′. These primers spanned a 239 bp sequence between residues 50 and 288. Following RT at 50 °C for 30 min (terminated by heating for 2 min at 94 °C), touchdown-PCR was performed for 10 cycles using the following temperatures: denaturation for 1 min at 94 °C, annealing for 2 min at 65 °C, with a lowering increment of 2 °C per cycle, and elongation for 3 min at 68 °C. Thermocycling was then continued for up to 21 cycles as follows: denaturation for 30 s at 94 °C, annealing for 30 s at 45 °C, and elongation for 45 s (plus 5 s per cycle) at 68 °C. Samples were collected at cycles 16–21 following the touchdown-PCR. All RT-PCR reactions were performed by the Mastercycler thermocycler (Eppendorf, Hamburg, Germany). The samples were separated on a 1.6 % agarose gel containing the SYBR Gold nucleic acid stain (Molecular Probes) and photographed under UV light. The attenuance of samples taken from cycles 16–21 were within a linear range.

Immunofluorescence

Cells fixed in methanol and treated with 3 % BSA were incubated first with mouse monoclonal antibodies against human H-FT (20 μg/ml) and subsequently with FITC-conjugated anti-mouse IgG and 1 μg/ml 4,6-diamidino-2-phenylindole (DAPI). Samples of 10 μl were loaded on to a glass slide and examined in an Olympus IX70 (Tokyo, Japan) fluorescence microscope ($\lambda_{excitation}$, 490 nm; $\lambda_{emission}$ 520 nm). DAPI-labelling assisted us in confirming that the FITC staining was cell-associated. Images were processed by EPIX's (Buffalo Grove, IL, U.S.A.) XCAP Image Acquisition, Display, Processing and Analysis Software. Quantitation of the data was performed by the Image-Pro Plus software (Media Cybernetics, Silver Spring, MD, U.S.A.).

LIP measurement and cell ROS production

LIP was measured by the calcein-based fluorescence method, as described previously [15]. ROS was determined in cells (10^6/ml) loaded with 10 μM H_2DCFDA-diAM for 20 min at 37 °C (based on the method described in [16]), centrifuged, and resuspended in Hepes-buffered saline supplemented with hydroxyethyl-starch-deferoxamine (BioMedical Frontiers, Minneapolis, MN, U.S.A.) in order to prevent extracellular-metal-catalysed substrate oxidation. Tracing of H_2O_2 (5 μM)-induced oxidation of the non-fluorescent carboxy-H_2DCF to the fluorescent carboxy-DCF was carried out fluorimetically ($\lambda_{excitation}$, 490 nm; $\lambda_{emission}$ 520 nm) (PTI, South Brunswick, NJ, U.S.A.). Maximum fluorescence attained in the sample (F_{max}) was obtained by cell permeabilization with 0.5 % Triton X-100 and addition of fresh 1 mM ferrous ammonium sulphate and 1 mM H_2O_2. The rate of ROS formation was assessed by the amount of carboxy-DCF produced per second. The concentration of carboxy-DCF is given by:

$$(\text{Carboxy-DCF})_c = (F/F_{max}) \times (\text{carboxy-DCF})_{cmax}$$

Where F and F_{max} are the fluorescence at any given time and the maximal fluorescence (both in relative units) respectively, and $(\text{carboxy-DCF})_{cmax}$ is the concentration factor obtained by calibration with standard carboxy-DCF. The concentration of carboxy-DCF in the cells $(\text{carboxy-DCF})_{in}$ was obtained from:

$$(\text{Carboxy-DCF})_{in} = (\text{carboxy-DCF})_c/(N_C \times V_C)$$

Where N_C is the cell concentration in the cuvette (cells/ml) and V_C is the volume of a single cell (ml/cell). Cells were counted in a Coulter counter and their volume obtained as described in [19].

Cellular iron content.

Total cell iron was measured as described in [12].

[^{55}Fe]Transferrin uptake and TfR surface expression

K562 cells (10^6/ml in Dulbecco's modified Eagle's medium supplemented with 20 mM Hepes and 1 mg/ml BSA) were exposed to 15 μg/ml of [^{55}Fe]transferrin alone (total) or with 1 mg/ml unlabelled tranferrin-Fe (non-specific) at 37 °C and 5 % CO_2. After 0 min, 30 min, 60 min and 120 min, the cells were transferred to ice, washed twice with cold PBS, stripped with

1 mg/ml Pronase E for 20 min, washed again, and resuspended in 200 μl of PBS. Triplicate aliquots (50 μl) were used for counting radioactivity in an aqueous Quicksafe A (Zinsser, Maidenhead, Berks., U.K.) fluid using a scintillation counter (Beckman, Irvine, CA, U.S.A.). Protein content was determined by the bicinchoninic acid method. Specific [^{55}Fe]transferrin uptake was obtained by subtracting the non-specific from the total counts for each time point. Cell surface TfR was measured as above, except that the cells were incubated at 4 °C and were not stripped.

RESULTS

Repression of ferritin subunits

Transfection of K562 cells with an antisense fragment reduced the cellular H-FT levels by approx. 50 % as compared with mock-transfected or untreated cells (Figure 1A and Table 1). The reduction in H-FT level was comparable with that attained by treatment with the iron chelator deferoxamine (50 μM for 24 h) (Figure 1A). However, unlike deferoxamine, which reduces the protein levels of both H-FT and L-FT (results not shown), H-FT antisense transfections evoked an increase in L-FT (Table 1), whereas H-FT levels were decreased. This indicates that the action of the antisense was not the result of a non-specific effect on the synthetic machinery of the cell. The blockage of H-FT expression by the H-FT antisense treatment was also assessed at the mRNA level. According to the RT-PCR analysis shown in Figure 1(B), the transfection significantly reduced the mRNA level of H-FT normalized to that of the housekeeping gene *L-7*. We tentatively attribute the mode of repression of H-FT to a reduction in the corresponding mRNA levels.

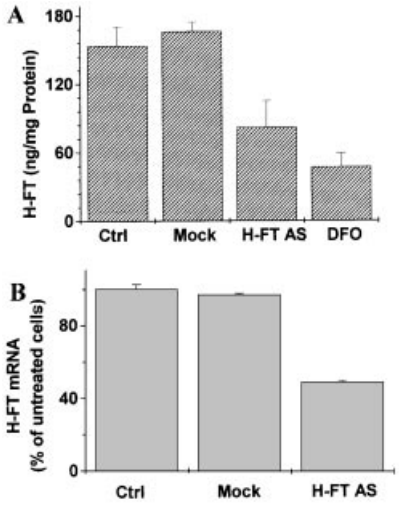

Figure 1 H-FT protein levels (A) and RT-PCR analysis of H-FT and L7 mRNA (B) in K562 cells transiently transfected with a partial human H-FT cDNA sequence transcribed in an antisense orientation

Ctrl, non-transfected cells; Mock, cells transfected with an 'empty' pRBG4 vector; H-FT AS, cells transfected with the antisense H-FT construct (samples were assayed 24 h following the transfection); deferoxamine (DFO), cells incubated for 24 h with 50 μM DFO. Each experiment was performed in triplicate and the results are expressed as the means of a representative experiment. Statistical analysis was done by independent Student's *t* test. H-FT level was reduced significantly ($P \leqslant 0.02$) by both H-FT antisense and DFO treatments. (**A**) Protein levels were determined by ELISA, as described in the Experimental section. (**B**) The relative changes in L7-normalized H-FT mRNA levels were calculated using densitometric analysis of bands of cycle 18, which were within the linear range of increase in luminosity against cycle number. Means $\pm$ S.D. of three independent experiments are shown. The mRNA density of the H-FT antisense-treated cells was significantly lower than that of the untreated cells ($P \leqslant 0.01$).

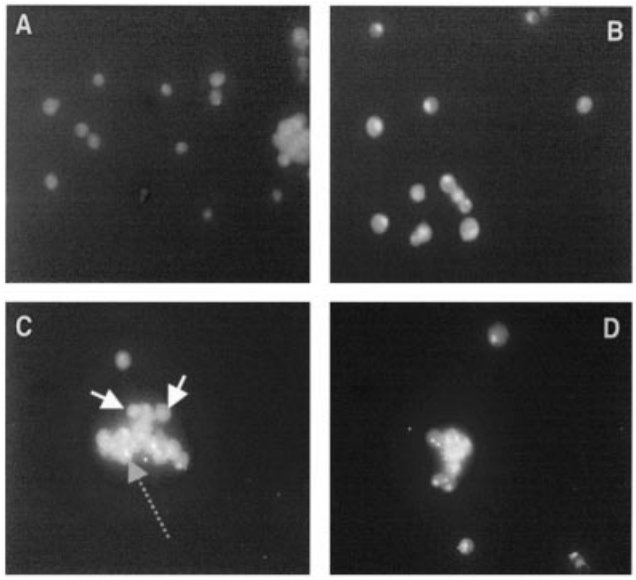

Figure 2 Immunofluorescence of H-FT levels in K562 cells

Cells were incubated for 1 h with mouse IgG (20 μg/ml) (**A**), or for 24 h with either: no additives (**B**), the pRBG4 plasmid into which a fragment of the H-FT cDNA was subcloned in an antisense orientation (**C**) or an 'empty' pRBG4 plasmid (**D**). Immunofluorescence was assayed by incubating the cells in (**B**–**D**) with mouse monoclonal antibodies against human H-FT. FITC-conjugated anti-mouse IgG served as secondary antibody in (**A**–**D**). Normal and broken-tailed arrows (**C**) indicate H-FT repressed and normal cells. Analysis of the attenuance (or light intensity 0–256 scale) was done on the four different cell treatments (**A**–**D**). Only cells in (**C**) showed a bimodal distribution of intensity (Gaussian 2 Peak fit, $P \leqslant 0.05$): in 7 out of 23 cells the average intensity was 122 ± 25 and in the remaining 16 out of 23 cells it was 186 ± 13. Magn. $\times 1000$.

Table 1 H-FT expression, LIP, pro-oxidant-induced ROS production and cellular iron content in K562 cells transiently transfected with H-FT AS

Cells were transfected using the DOTAP reagent, and assayed in parallel 24 h later for the indicated parameters. H-FT and L-FT expression were determined by the ELISA described in the Experimental section. The pre-normalized levels of FT in the untreated cells were 157 ± 16 ng/mg and 39 ± 6 ng/mg protein for H-FT and L-FT respectively. The control levels varied among experiments within the ranges of 140–400 ng/mg and 30–150 ng/mg protein for H-FT and L-FT respectively. LIP levels were measured by the calcein method [15] and normalized to intracellular calcein. LIP levels in untreated cells were 1.5 ± 0.002 μM (normalized to 100 %). Those values varied among experiments within the range of 0.08–0.14 μM. ROS production was determined by the carboxy-DCF method, subsequent to a 5 μM H_2O_2 challenge, as described in the Experimental section. Its level in the untreated cells was $5.7 \pm 9.7 \times 10^{-4}$ nM carboxy-DCF oxidized per s (normalized to 100 %). *Values for the ferritin antisense-transfected cells were significantly different from the values for untreated cells ($P \leqslant 0.01$), as determined by Student's independent *t* test. †Values are given as percent of untreated cells and are expressed as means $\pm$ S.D. of three replicates of a representative experiment.

Transfection vector	H-FT†	L-FT†	Normalized LIP†	ROS production†	Iron content (μM)
None	100 ± 10	100 ± 19	100 ± 0.14	100 ± 0.14	1088 ± 407
pRBG4	106 ± 5	119 ± 3	102 ± 0.14	123 ± 7	799 ± 372
pRBG4 + H-FT antisense	52 ± 15*	220 ± 32*	149 ± 0.28*	646 ± 68*	735 ± 225

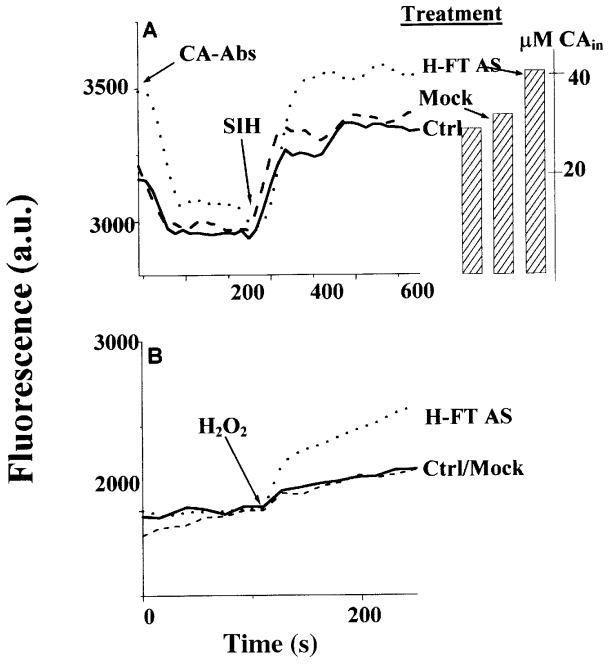

Figure 3 LIP levels and ROS production in H-FT-repressed cells

(**A**) Determination of LIP in K562 cells. Following quenching of non-cell-associated calcein (CA) fluorescence by anti-CA antibodies (Abs), the permeable chelator salicylaldehyde isonicotinoyl hydrazone (SIH) was added, and LIP was determined as described in [15] from the stabilized signal attained after SIH addition. Cell incubations prior to LIP determination: dotted line, 24 h, no treatment; solid line, mock-transfected cells; broken line, cells transfected with an H-FT cDNA fragment in an antisense (AS) orientation. The bars represent concentrations of calcein (μM) in the cells following the addition of the chelator SIH. (**B**) Determination of pro-oxidant-induced ROS formation in K562 cells. ROS production was determined based on the rise in fluorescence in H_2DCFDA-diAM-loaded cells, as described in the Experimental section. H_2O_2 (5 μM) was used as the pro-oxidant, and was added to the cells where indicated. Treatment annotations are the same as in (**A**).

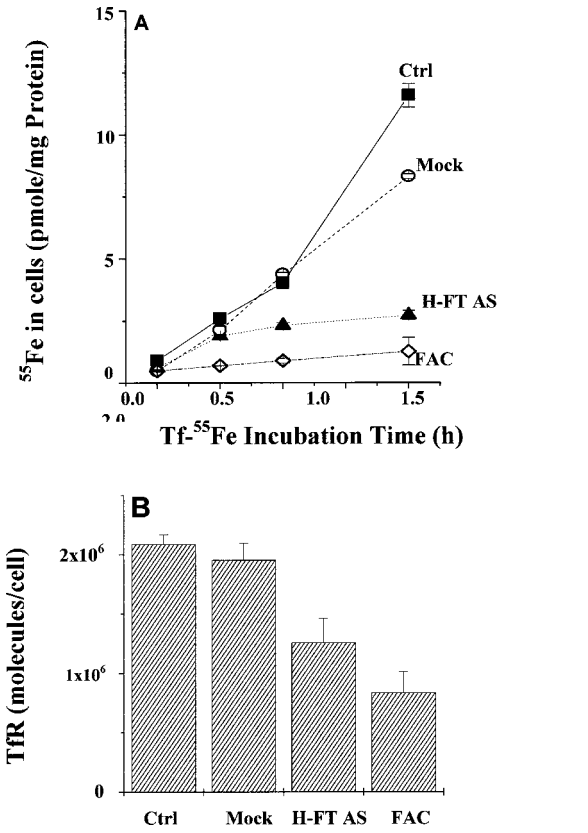

Figure 4 [^{55}Fe]Transferrin uptake (A) and TfR surface expression (B) in cells transfected with a fragment of H-FT in an antisense orientation

(**A**) Following the specified treatments, uptake of [^{55}Fe]transferrin and surface expression of TfR were assayed as described in the Experimental section. The treatments in (**A**) were: none (■), mock transfection with an empty plasmid (○), transfection with a plasmid carrying a part of H-FT's cDNA in an antisense orientation (▲) and ferric ammonium citrate (◇) (20 μM for 24 h). (**B**) TfR surface expression following H-FT antisense transfection and ferric amonium citrate (FAC) treatment was significantly different ($P \leqslant 0.02$) from the untreated cells as determined by Student's independent t test. A representative experiment performed in triplicate is presented in both (**A**) and (**B**).

Although substantial, the level of antisense repression of H-FT expression was not complete in the experimental conditions used. It was, therefore, of interest to ascertain whether the antisense affected the cells differentially. In order to address this issue, we used indirect immunofluorescence staining of cells with H-FT antibodies. All staining was confirmed to be cell-associated, by both phase-contrast and immunofluorescent microscopy, which showed co-localization of the FITC stain with the nuclear stain DAPI (results not shown). A quantitative analysis of the fluorescent intensity associated with transfected cells revealed a bimodal distribution: in two-thirds of the cells, the average intensity (in 0–256 scale) was 123 ± 25, whereas in the remaining third it was 186 ± 13. The latter corresponded to the average intensity obtained in non-transfected cells, whereas the former corresponded to the value obtained in transfected cells in which treatment with the primary anti-H-Ft antibody was omitted. The results agree with the possibility that H-FT was repressed only in that fraction of cells that was successfully transfected (Figure 2). Therefore the cellular parameters affected by the antisense transfection should be regarded as underestimates when expressed as means of the whole cell population.

Effects of H-FT repression on LIP and ROS formation

The effects of the H-FT antisense on the expression of H-FT and L-FT could be attributed to two possible mechanisms: one involving a direct, but opposing, action of antisense on each subunit, and the other based on the specific repression of the H-FT subunit, indirectly leading to increased L-FT synthesis by increasing the LIP, and thereby decreasing the IRP activity. Our results (Table 1) support the second mechanism. The experimental steady-state levels of LIP were significantly higher in the H-FT antisense-transfected cells as compared with either untreated cells or mock-transfected cells (Table 1 and Figure 3A). These effects are consistent with the reduction in L-FT observed in cells overexpressing H-FT in which LIP was reduced [13,20]. In parallel, higher ROS production was observed after the H-FT antisense-transfected cells were challenged with H_2O_2 (5 μM) (Figure 3B). This result indicates that the up-modulation of LIP by the H-FT antisense transfection is associated with a catalytic (labile) reservoir. Although the LIP levels in cells with different H-FT levels were significantly different, their total iron content was apparently similar (Table 1). It should be emphasized that LIP is the metabolically active cellular iron, even though it constitutes only a minor fraction ($< 1\%$) of the total cellular iron (results not shown and [12]).

Effects of H-FT repression on TfR

The possibility that the rise in LIP evoked by H-FT repression led to IRP inactivation [21,22], and thereby increased L-FT expression, was also assessed in terms of TfR expression, i.e. TfR-mediated iron uptake (Figure 4A) and TfR surface expression (Figure 4B). H-FT repression, like addition of an iron salt (ferric ammonium citrate, 20 μM for 24 h), repressed both transferrin-Fe uptake and TfR expression. This supports the notion that the repressive effect of the H-FT antisense on TfR was via up-modulation of the LIP.

DISCUSSION

We have used transient transfection of an H-FT antisense fragment in order to directly assess H-FT's role as a regulator of LIP and ROS formation. It has been generally assumed that ferritin protein expression is regulated translationally by IRP activity, which is controlled by the LIP levels [21,22]. However, ferritin has also been proposed to function as an 'active' modulator of the LIP by IRP-independent mechanisms associated with transcriptional regulation [5,23,24]. In order to ascertain that ferritin expression can actively affect the LIP, we aimed to set up experimental conditions that allowed ferritin levels to be monitored independently of the LIP. We achieved that goal by specifically reducing H-FT expression, using transient transfection with an H-FT antisense fragment (Figure 1A and Table 1). The reduction in the average cellular H-FT levels was substantial (approx. 50 %). However, only about two-thirds of the cells underwent transfection (Figure 2). Thus the actual changes evoked in the transfected sub-population are 25 % higher than the average value for the entire population, representing 75 % reduction in H-FT in the transfected sub-population.

The reduction in H-FT levels evoked a concomitant increase in the LIP, whether measured directly with a fluorescent sensor or indirectly by its capacity to promote ROS formation or induce synthesis of the L-FT subunit (Table 1). The mechanism by which repression of H-FT affected the LIP differed from that of chelators which act on the LIP–IRP feedback loop. Thus unlike iron chelation by deferoxamine, which reduces both ferritin subunit levels via reduction in the LIP and activation of IRP, the H-FT antisense transfection led to an increase in the steady-state LIP and associated parameters. Moreover, the fact that the transfected cells expressed reduced H-FT content, despite their demonstrably higher LIP levels, indicates that repression of H-FT by antisense-mediated transfection overcame the cell IRP regulatory capacity [21,22].

These results complement studies in which ferritin was overexpressed independently of LIP, using cells stably transfected with H-FT mutated in its iron-responsive element [12–14]. In those studies, overexpression of H-FT led to a concomitant decrease in LIP, supporting the presumed role of ferritin in controlling LIP levels. Taken as a whole, the modulation of H-FT expression by transfections with H-FT constructs provides experimental support for the active role of ferritin in both up- and down-regulation of LIP and ROS generation. This active role of ferritin has been implied in different aspects of cell growth [25], such as protection against oxidative stress [26–28], intracellular pathogens [29–31], and in various inflammatory conditions [30–32]. An active role of H-FT in the control of LIP levels provides an experimental framework for rationalizing the observed oncogene-mediated transcriptional repression of H-FT [1–6,33]. Such a repression has been hypothesized to support cell proliferation, presumably by making more LIP available for accelerated cell growth. However, this study provides the first experimental evidence linking the presumed rise in LIP to H-FT repression. Unfortunately the delayed expression of the ferritin antisense in transfected cells hampered the assessment of the role of ferritin in accelerated cell growth. This subject is currently under investigation with the aid of antisense oligodeoxynucleotides that allow long-term studies in culture (O. Kakhlon, Y. Gruenbaum and Z. I. Cabantchik, unpublished work).

REFERENCES

1 Bevilacqua, M. A., Faniello, M. C., Quaresima, B., Tiano, M. T., Giuliano, P., Feliciello, A., Avvedimento, V. E., Cimino, F. and Costanzo, F. (1997) A common mechanism underlying the E1A repression and the cAMP stimulation of the H ferritin transcription. J. Biol. Chem **272**, 20736–20741

2 Bevilacqua, M. A., Faniello, M. C., Russo, T., Cimino, F. and Costanzo, F. (1998) P/CAF/p300 complex binds the promoter for the heavy subunit of ferritin and contributes to its tissue-specific expression. Biochem. J. **335**, 521–525

3 Tsuji, Y., Kwak, E., Saika, T., Torti, S. V. and Torti, F. M. (1993) Preferential repression of the H subunit of ferritin by adenovirus E1A in NIH-3T3 mouse fibroblasts. J. Biol. Chem. **268**, 7270–7275

4 Tsuji, Y., Akebi, N., Lam, T. K., Nakabeppu, Y., Torti, S. V. and Torti, F. M. (1995) FER-1, an enhancer of the ferritin H gene and a target of E1A-mediated transcriptional repression. Mol. Cell. Biol. **15**, 5152–5164

5 Tsuji, Y., Moran, E., Torti, S. V. and Torti, F. M. (1999) Transcriptional regulation of the mouse ferritin H gene. Involvement of p300/CBP adaptor proteins in FER-1 enhancer activity. J. Biol. Chem. **274**, 7501–7507

6 Wu, K. J., Polack, A. and Dalla Favera, R. (1999) Coordinated regulation of iron-controlling genes, H-ferritin and IRP2, by c-MYC. Science (Washington, D.C) **283**, 676–679

7 Fahmy, M. and Young, S. P. (1993) Modulation of iron metabolism in monocyte cell line U937 by inflammatory cytokines: changes in transferrin uptake, iron handling and ferritin mRNA. Biochem. J. **296**, 175–181

8 Miller, L. L., Miller, S. C., Torti, S. V., Tsuji, Y. and Torti, F. M. (1991) Iron-independent induction of ferritin H chain by tumor necrosis factor. Proc. Natl. Acad. Sci. U.S.A. **88**, 4946–4950

9 Rogers, J. T., Bridges, K. R., Durmowicz, G. P., Glass, J., Auron, P. E. and Munro, H. N. (1990) Translational control during the acute phase response. Ferritin synthesis in response to interleukin-1. J. Biol. Chem. **265**, 14572–14578

10 Tsuji, Y., Miller, L. L., Miller, S. C., Torti, S. V. and Torti, F. M. (1991) Tumor necrosis factor-alpha and interleukin 1-alpha regulate transferrin receptor in human diploid fibroblasts. Relationship to the induction of ferritin heavy chain. J. Biol. Chem. **266**, 7257–7261

11 Wei, Y., Miller, S. C., Tsuji, Y., Torti, S. V. and Torti, F. M. (1990) Interleukin 1 induces ferritin heavy chain in human muscle cells. Biochem. Biophys. Res. Commun. **169**, 289–296

12 Epsztejn, S., Glickstein, H., Picard, V., Slotki, I. N., Breuer, W., Beaumont, C. and Cabantchik, Z. I. (1999) H-ferritin subunit overexpression in erythroid cells reduces the oxidative stress responses and induces multidrug resistance properties. Blood **94**, 1–12

13 Picard, V., Epsztejn, S., Santambrogio, P., Cabantchik, Z. I. and Beaumont, C. (1998) Role of ferritin in the control of the labile iron pool in murine erythroleukemia cells. J. Biol. Chem. **273**, 15382–15386

14 Cozzi, A., Corsi, B., Levi, S, Santambrogio, P., Albertini, A. and Arosio, P. (2000) Overexpression of wild type and mutated human ferritin H-chain in HeLa cells: *in vivo* role of ferritin ferroxidase activity. J. Biol. Chem. **275**, 25122–25129

15 Epsztejn, S., Kakhlon, O., Glickstein, H., Breuer, W. and Cabantchik, I. (1997) Fluorescence analysis of the labile iron pool of mammalian cells. Anal. Biochem. **248**, 31–40

16 Breuer, W., Greenberg, E. and Cabantchik, Z. I. (1997) Newly delivered transferrin iron and oxidative cell injury. FEBS Lett. **403**, 213–219

17 Breuer, W., Epsztejn, S. and Cabantchik, Z. I. (1995) Iron acquired from transferrin by K562 cells is delivered into a cytoplasmic pool of chelatable iron(II). J. Biol. Chem. **270**, 24209–24215

18 Lee, B. S., Gunn, R. B. and Kopito, R. R. (1991) Functional differences among nonerythroid anion exchangers expressed in a transfected human cell line. J. Biol. Chem. **266**, 11448–11454

19 Slotki, I. N., Breuer, W. V., Greger, R. and Cabantchik, Z. I. (1993) Long-term cAMP activation of Na(+)-K(+)-2Cl- cotransporter activity in HT-29 human adenocarcinoma cells. Am. J. Physiol. **264**, C857–C865

20 Picard, V., Renaudie, F., Porcher, C., Hentze, M. W., Grandchamp, B. and Beaumont, C. (1996) Overexpression of the ferritin H subunit in cultured erythroid cells changes the intracellular iron distribution. Blood **87**, 2057–2064

21 Klausner, R. D., Rouault, T. A. and Harford, J. B. (1993) Regulating the fate of mRNA: the control of cellular iron metabolism. Cell (Cambridge, Mass.) **72**, 19–28

22 Theil, E. C. (1994) Iron regulatory elements (IREs): a family of mRNA non-coding sequences. Biochem. J. **304**, 1–11
23 Elia, G., Polla, B., Rossi, A. and Santoro, M. G. (1999) Induction of ferritin and heat shock proteins by prostaglandin A1 in human monocytes. Evidence for transcriptional and post-transcriptional regulation. Eur. J. Biochem. **264**, 736–745
24 Pham, D. Q., Winzerling, J. J., Dodson, M. S. and Law, J. H. (1999) Transcriptional control is relevant in the modulation of mosquito ferritin synthesis by iron. Eur. J. Biochem. **266**, 236–240
25 Weinberg, E. D. (1992) Iron depletion: a defense against intracellular infection and neoplasia. Life Sci. **50**, 1289–1297
26 Balla, G., Jacob, H. S., Balla, J., Rosenberg, M., Nath, K., Apple, F., Eaton, J. W. and Vercellotti, G. M. (1992) Ferritin: a cytoprotective antioxidant strategem of endothelium. J. Biol. Chem. **267**, 18148–18153
27 Balla, J., Jacob, H. S., Balla, G., Nath, K., Eaton, J. W. and Vercellotti, G. M. (1993) Endothelial-cell heme uptake from heme-proteins: Induction of sensitization and desensitization to oxidant damage. Proc. Natl. Acad. Sci. U.S.A. **90**, 9285–9289
28 Cairo, G., Tacchini, L., Pogliaghi, G., Anzon, E., Tomasi, A. and Bernelli-Zarzera, A. (1995) Induction of ferritin synthesis by oxidative stress. Transcriptional and post-transcriptional regulation by expansion of the ''free'' iron pool. J. Biol. Chem. **270**, 700–703
29 Brock, J. H. (1994) Iron and the immune system. In Iron and Human Disease (Lauffer, R. B., ed.), pp. 161–178, CRC Press, Boca Raton, Ann Arbor, London, Tokyo
30 Brock, J. H. (1994) Iron in infection, immunity, inflammation and neoplasia. In Iron Metabolism in Health and Disease (Brock, J. H., Halliday, J. W., Pippard, M. P. and Powell, L. W., eds.), pp. 354–389, W. B. Saunders, London
31 Konijn, A. M. (1994) Iron metabolism in inflammation. In Baillere's Clinical Haematology: Clinical Disorders of Iron Metabolism (Hershko, C., ed.), pp. 829–850, Baillere Tindall, London
32 Konijn, A. M. and Hershko, C. (1977) Ferritin synthesis in inflammation. I. Pathogenesis of impaired iron release. Br. J. Haematol. **37**, 7–16
33 Fuhrmann, G., Rosenberger, G., Grusch, M., Klein, N., Hofmann, J. and Krupitza, G. (1999) The MYC dualism in growth and death. Mutat. Res. **437**, 205–217

Received 7 February 2001/19 March 2001; accepted 9 April 2001